



Removal of Ni²⁺, Cu²⁺, Zn²⁺, Cd²⁺ and Pb²⁺ ions from aqueous solutions using cashew peduncle bagasse as an eco-friendly biosorbent

Sarah Abreu Moreira^a, Diego Quadros Melo^{b,*}, Ari C. Alves de Lima^a, Francisco Wagner Sousa^a, André Gadelha Oliveira^b, André Henrique B. Oliveira^b, Ronaldo Ferreira Nascimento^b

^aDepartamento de Engenharia Hidráulica e Ambiental, Universidade Federal do Ceará, Campus do Pici, Centro de Tecnologia, Bloco 713-CEP: 60455-900, Fortaleza, Ceará, Brazil, emails: sarahbreu@yahoo.com.br (S.A. Moreira), ari072000@yahoo.com.br (A.C.A. de Lima), fr.wagner@gmail.com (F.W. Sousa)

^bLaboratório de Análise Traço, Departamento de Química Analítica e Físico Química, Universidade Federal do Ceará, Campus do Pici, Centro de Ciências, Bloco 940-CEP: 60451-970, Fortaleza, Ceará, Brazil, emails: diegodqm@gmail.com (D.Q. Melo), titogadelha@yahoo.com.br (A.G. Oliveira), andrehbo@yahoo.com.br (A.H.B. Oliveira), ronaldo@ufc.br (R.F. Nascimento)

Received 6 August 2014; Accepted 25 March 2015

ABSTRACT

In this study, the adsorption efficiency of cashew peduncle bagasse (CPB) is reported for the removal of single-(mono-) and multi-metal ions (Cd²⁺; Cu²⁺; Ni²⁺; Pb²⁺; and Zn²⁺) from synthetic and natural effluents using fixed-bed columns. The percentage of saturation realised in this study using a mono-elemental system was as follows: Pb²⁺ > Cd²⁺ > Zn²⁺ > Ni²⁺ > Cu²⁺. The metal ion recovery rate was determined by column elution; we demonstrated 100% metal ion recovery using 40 mL of HCl or HNO₃ (0.1 mol L⁻¹) as the eluent, with the exception of Pb²⁺. The adsorbent regeneration process decreased the removal efficiencies to 90% (Pb²⁺), 44% (Cu²⁺), 99% (Ni²⁺), 81% (Cd²⁺) and 74% (Zn²⁺) after the first cycle. The breakthrough curves and kinetic adsorption factors controlling the adsorption process were also studied. The Thomas model has produced the best fit with the experimental data.

Keywords: Cashew peduncle bagasse; Multi-metal adsorption; Column adsorption; Biosorbent regeneration

1. Introduction

In recent years, increased industrial activities have intensified environmental hazards related to metal pollution and ecosystems are known to have deteriorated due to the accumulation of dangerous heavy metal pollutants [1]. Heavy metals have been used in various industrial processes due to their technological

importance. In addition, inefficient treatment of wastewaters from these industries may introduce a greater human and environmental exposure. Traditional technologies, such as chemical precipitation, ion exchange, activated carbon adsorption and membrane separation processes have been applied widely for the removal of heavy metals from contaminated waters [2,3]. However, these processes involve high operation and capital costs [4].

*Corresponding author.

Adsorption, particularly, is one of the most promising techniques used to remove metal ions from water. Among the adsorbents used for water decontamination, lignocellulose-derived materials are often selected, due to their low cost and simplicity, unlike activated carbon. Moreover, there is a growing worldwide interest in the use of natural fibres [5–7] as adsorbents, including banana [8,9], coconut green bagasse [10–13], sugar cane bagasse [14–16] and cashew peduncle bagasse (CPB) [17,18].

The last adsorbent deserves particular mention, as the production of cashew peduncle is concentrated in the north-east region of Brazil and amounts to approximately 1.5 million tons per year, with 90–94% of the final product unused. The peduncle-processing industry has applications in the manufacture of drinks, sweets, jams, nectar, flour, fermented products and food ration production, but less than 6% of the available peduncle product is used [19]. There are several major advantages in using natural fibres as adsorbents, including the ready availability of renewable sources in nature, low cost associated with its generation, biodegradability and excellent mechanical properties.

Wastewaters usually contain multiple metal ions, which may cause interference and competition effects, depending on the concentration of metals competing for binding sites in an adsorbent. However, most studies on low-cost adsorbents have been conducted using either a single or binary solution of metal ions [20–23].

Therefore, studies assessing the competitive adsorption of metal ions from solutions are necessary for improving the design of wastewater treatment systems, which may be outdated. Single- and multi-metal ion adsorption have been investigated with low-cost adsorbents using a batched system [24,25] but few applications have been developed using fixed-bed column operations [26].

In this study, the adsorption efficiency of CPB was investigated for removal and recovery of toxic ions (Cd^{2+} , Cu^{2+} , Ni^{2+} , Pb^{2+} and Zn^{2+}) from synthetic and industrial effluent through continuous system. The effects of different parameters, such as column bed depth and flow rate were investigated using a laboratory scale fixed-bed column. Thomas model was analysed to study the dynamic behaviour of the column.

2. Material and methods

2.1. Biosorbent characterisation

2.1.1. SEM analysis

Surface morphology was studied by scanning electron microscopy (SEM) using a model DSM 960/Zeiss

with a 20 kV electron beam. The sample was coated with gold (sputter coater) in argon plasma (model BAL.ZERS 5CD50).

2.1.2. Infrared spectroscopy (FTIR)

Infrared spectroscopy (FTIR Prestige apparatus of Shimadzu) was performed to identify the main functional groups present on the adsorbent surface [27,28]. The samples were prepared by mixing 1 mg of material with 99 mg of spectroscopy grade KBr (Merck, São Paulo).

2.1.3. X-ray fluorescence

X-ray fluorescence (XRF) measurements were performed on cashew peduncle bagasse using a wavelength-dispersive X-ray fluorescence spectrometer (Rigaku ZSX Mini II) equipped with a Pd anode X-ray tube and operated at 40 kV and 1.2 mA.

2.2. Reagent and solutions

Analytical grade reagents (Merck) were used for preparing different concentrations of synthetic solutions. Standard stock solutions of each metal ion, i.e. Pb^{2+} , Cu^{2+} , Ni^{2+} , Zn^{2+} and Cd^{2+} , were prepared in distilled water at pH 5.0 and a concentration of 1,000 mg L⁻¹. A multi-element solution was also prepared in distilled water at pH 5.0 by dissolving $\text{Pb}(\text{NO}_3)_2 \cdot \text{H}_2\text{O}$, $\text{Cu}(\text{NO}_3)_2 \cdot 6\text{H}_2\text{O}$, $\text{Ni}(\text{NO}_3)_2 \cdot 6\text{H}_2\text{O}$, $\text{Zn}(\text{NO}_3)_2 \cdot 6\text{H}_2\text{O}$ and $\text{Cd}(\text{NO}_3)_2 \cdot 6\text{H}_2\text{O}$.

Acetate buffer was prepared with sodium acetate (CH_3COONa) and glacial acetic acid (CH_3COOH) (VETEC, São Paulo, Brazil). NaOH (0.10 mol L⁻¹) and HCl (0.10 mol L⁻¹) solutions were used for pH adjustments.

2.3. Preparation of the cashew peduncle bagasse adsorbent

The cashew peduncle bagasse was supplied by Embrapa Tropical Agro-industry, (EMBRAPA-CE-BRAZIL). The CPB was treated with a 0.1 mol L⁻¹ NaOH solution for 3 h at room temperature ($28 \pm 2^\circ\text{C}$). Afterwards, the CPB was washed with deionised water and acetate buffer solution (pH 5.0) and dried at room temperature. The particle size used in this study was in the range of 60 to 99 mesh.

2.4. Experimental adsorption

2.4.1. Column studies

Column adsorption experiments were conducted using active CPB (pretreated with an alkaline solution).

Fixed-bed biosorption studies were performed in polyethylene columns with a 1.1 cm internal diameter and a 30.0 cm height. For the continuous flow experiments, a synthetic multi-metal ion solution (approximately 100.0 mg L⁻¹) was pumped downwards through the CPB-packed column using a peristaltic pump (model MINIPULS 3, GILSON). The flow rates tested were 3.0 and 6.0 mL min⁻¹. The effect of the adsorbent height was also evaluated for heights of 8.0 and 12.0 cm. The breakthrough curves for the single-(mono-) and multi-metal ion solutions were obtained by plotting C/C_0 vs. volume. Column effluent aliquots of 10.0 mL were collected, and the ion concentrations were determined.

The metal residual concentration was determined by an atomic absorption spectrophotometer, model GBC 933 *plus*, Australia. All experiments were carried out twice.

2.4.2. Column data analysis

To determine the performance of adsorption column, time for breakthrough appearance and the shape of the breakthrough curve are important factors. Breakthrough curves were determined as the relationship between the concentration of the sample that had passed through the adsorbent and the initial concentration. For an ideal breakthrough curve, C_0 is the effluent adsorbate concentration, and V_x is the effluent volume that percolated through the column. The breakpoint (C_b) occurs when the effluent concentration reaches 5% of the initial concentration (C_0). The column reaches complete saturation when the concentration, C_x , approaches the initial concentration, C_0 . The total effluent volume, V_b , is equal to the volume eluted through the column until the breakpoint is established. The part between C_x (exhaustion point) and C_b (breakpoint) is called the primary adsorption zone (PAZ), and the time (t_x) is PAZ (min), is calculated by Eq. (1) [29,30]:

$$t_x = \frac{V_x}{F_m} \quad (1)$$

where F_m is the flow rate (mL min⁻¹) and V_x is the exhaustion volume (mL).

The time (t_δ) required for the movement of PAZ downwards in the column given by Eq. (2) [30]:

$$t_\delta = \left(\frac{V_x - V_b}{F_m} \right) \quad (2)$$

where V_b is the breakthrough volume (mL), V_x is the exhaustion volume (mL) and F_m is the flow rate (mL min⁻¹).

The time required to achieve PAZ is given by Eq. (3) [29,30]:

$$t_f = (1 - f)t_\delta \quad (3)$$

where t_f is the time of PAZ formation and f is the fractional capacity of adsorbent in the adsorption zone, which is characterised by removal of the solute from the solution under limiting conditions.

The adsorbent fractional capacity (f) is given by Eq. (4) [29,30]:

$$f = \frac{\int_{V_b}^{V_x} (C_0 - C)}{C_0(V_x - V_b)} dv \quad (4)$$

Thus, for depth, D , of the adsorbent, the depth and time ratios are given by Eq. (5):

$$\frac{\delta}{D} = \frac{t_\delta}{(t_x - t_f)} \quad (5)$$

where δ is the PAZ length (cm), and D is the adsorbent depth (cm).

The column saturation percentage is obtained by Eq. (6):

$$\% \text{ saturation} = \left[1 - \frac{\delta(f - 1)}{D} \right] \times 100 \quad (6)$$

The maximum capacity of toxic metal ion removal by the column is given by Eq. (7) [30]:

$$Q = \frac{C_0 x V}{m_s} \int_{t=0}^{t=x} \left(1 - \frac{C}{C_0} \right) dt \quad (7)$$

where Q is the maximum adsorption capacity (mg g⁻¹), C_0 and C are the initial concentrations of the solution and the metal ion in a determined volume (mg L⁻¹), respectively, m_s is the adsorbent mass (g), V is the flow rate (L min⁻¹) and t is the time (min).

2.4.3. Thomas model

The Thomas model is one of the most general and widely used methods in column performance theory. This model determines the maximum solid-phase concentration, where external and internal diffusion

are limiting steps. The Thomas model is expressed by Eq. (8) [31]:

$$\frac{C}{C_0} = \frac{1}{1 + \exp\left[\frac{K_t(q_0 m_s - C_0 V_e)}{F_m}\right]} \quad (8)$$

where C is the adsorbate concentration in a specific volume, C_0 is the initial solution concentration (mg L^{-1}), K_t is the kinetic adsorption rate constant ($\text{L min}^{-1} \text{mg}^{-1}$), q_0 is the maximum solid-phase concentration (mg g^{-1}) at the maximum adsorption capacity, m_s is the amount of biosorbent (g), F_m is the volumetric flow rate (L min^{-1}), and V_e is the effluent volume (L).

The adsorption capacity of the bed, q_0 , and the Thomas constant, K_t , can be obtained from the intercept and slope, respectively, of a curve obtained by plotting $\ln(C/C_0 - 1)$ as a function of $V_e/F_m = t$ or as a function of V_e from the breakthrough point, C_b , until exhaustion point, C_x . These constants can be obtained using non-linear regression analysis. The Thomas model can be linearised as Eq. (9):

$$\ln\left(\frac{C_0}{C} - 1\right) = \frac{K_t q_0 m_s}{F_m} - \frac{K_t C_0 V_e}{F_m} \quad (9)$$

2.4.4. Column regeneration and experiments with effluent from the electroplating industry

Sample volumes of 250 mL containing 100.0 mg L^{-1} of Pb^{2+} , Cu^{2+} , Ni^{2+} , Zn^{2+} and Cd^{2+} were applied to the CPB-packed column using a previously described methodology. After application of the sample to the column, the column was eluted with 50 mL of 1.0 mol L^{-1} HCl and 1.0 mol L^{-1} HNO_3 . Aliquots of 10.0 mL were collected and the ion concentrations were determined before and after the adsorption process.

Samples were applied to the column five times, and for each cycle, 50 mL of water, 250 mL of multi-metal solution and 50 mL hydrochloric acid (1.0 mol L^{-1}) were used for metal ion desorption.

A natural effluent obtained from the electroplating industry (Fortaleza, CE, Brazil) was studied to determine the best conditions for the fixed-bed biosorption process.

3. Results and discussion

3.1. Biosorbent characterisation

The adsorbent studied is a natural polymer composed mainly of cellulose, hemicellulose and lignin in

different proportions. Alkali treatment causes the change in configuration of cellulose which causes an increased availability of active sites for adsorption. Therefore, the main functional groups were observable by absorption spectra in the infrared region, as shown in Fig. 1(a). It can observe an absorption range of polysaccharides in a broad band between $3,100$ and $3,500 \text{ cm}^{-1}$. The bands at $3,535$ and $3,371 \text{ cm}^{-1}$ are indicative of stretching due to the presence of $-\text{OH}$ and $-\text{NH}$ functional groups, whereas the bands at $2,921$ and $2,928 \text{ cm}^{-1}$ are characteristic of $\text{C}-\text{H}$ functional groups that result in the stretching apparent in fibres including cellulose, hemicellulose and lignin. The absorption band at $1,650$ to $1,736 \text{ cm}^{-1}$ was assigned to $\text{C}=\text{O}$ groups found in carboxylic acid, ketones, aldehydes, esters and carbonyl [32]. The band observed at $1,557 \text{ cm}^{-1}$ can be attributed to amines and amides groups, and the bands at $1,036$ and

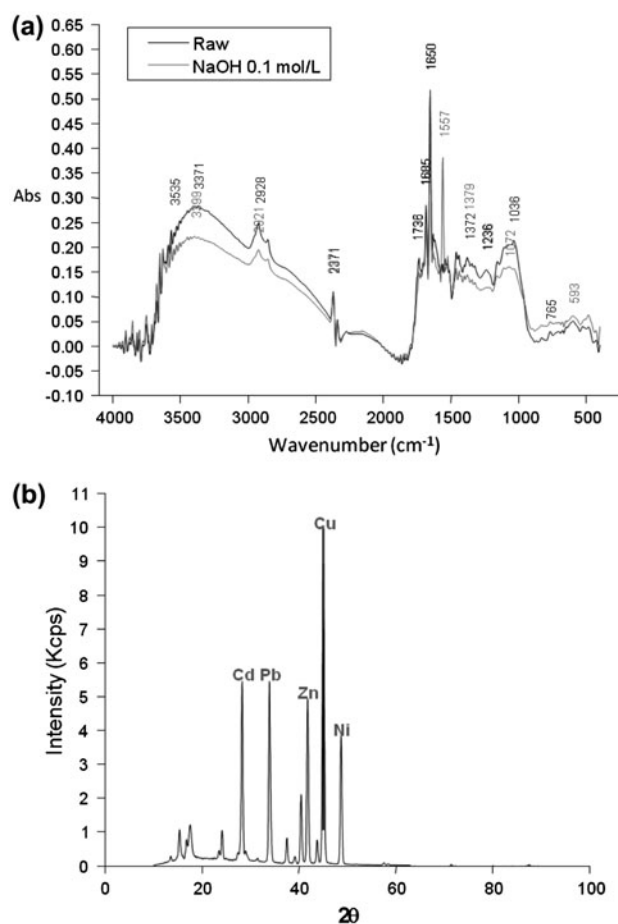


Fig. 1. Infrared spectra of the cashew peduncle bagasse before and after treatment with $\text{NaOH } 0.1 \text{ mol L}^{-1}$ (a). X-ray fluorescence spectra of the metals adsorbed onto the cashew peduncle bagasse that had been treated with an alkaline solution (b).

1,072 cm^{-1} are characteristic of C–O alcohol groups. The bands of the C=O groups were more intense than those of the C–O groups, likely due to the presence of a greater number of C=O groups in the biosorbent. The vibrational modes after chemical treatment have not significantly changed, and the main bands appeared approximately in the same range as the wave numbers. The functional groups observed in the treated and untreated materials were primarily responsible for metal adsorption from the tested solution.

XRF measurements were performed to obtain information about the metal ions present on the adsorbent surface fibres (Fig. 1(b)). Raw CPB was analysed for adsorbed metal ions after chemical treatment (Table 1). Pb^{2+} , Cd^{2+} and Ni^{2+} ions were not observed in this sample. Following treatment with the multi-metal ion solution, analysis of the fibre demonstrated increased Cu^{2+} (from 1.78 to 29.21%) and Zn^{2+} (1.84 to 10.69%) ion retention. These results suggest that the fibre adsorbed these ions from solution in the presence of Pb^{2+} (37.40%), Cd^{2+} (7.55%) and Ni^{2+} (10.51%) ions at a range of concentrations, as shown in Fig. 2(b) and the data presented in Table 1. Additionally, all the other ions present in the raw CPB (without chemical modification) had their quantities reduced after chemical treatment. The K^+ (35.42%) and Ca^{2+} (27.19%) ions comprised the majority of the ions present in the raw fibre, and these values changed to 1.63 and 0.83%, respectively, after treatment. This suggests that one type of metal is removed by ion-exchange mechanism.

To obtain more information about the surface structure of these samples, SEM micrographs of the

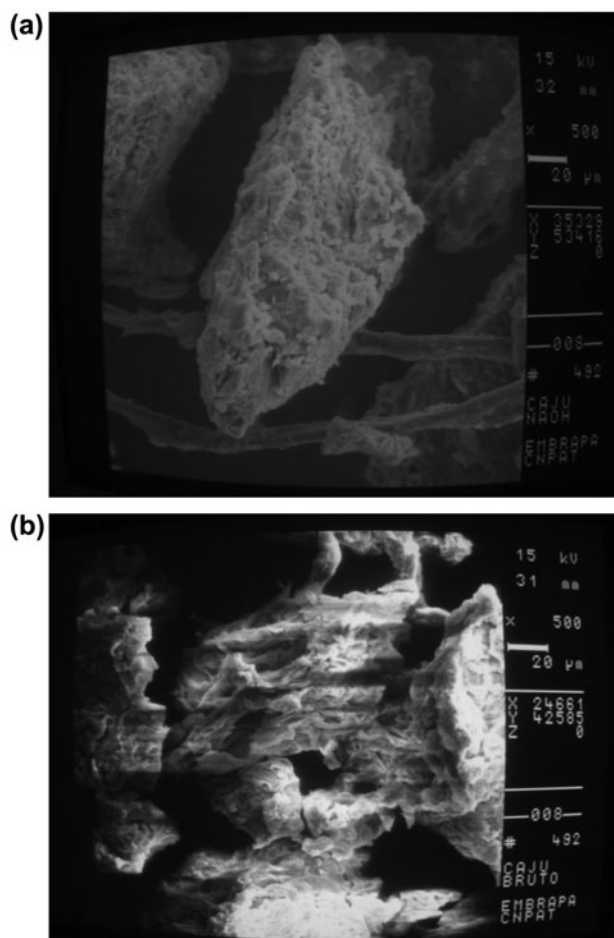


Fig. 2. SEM image of the cashew peduncle bagasse with particle sizes in the range of a 20–59 mesh (500 \times). Both untreated (a) and treated (b) with NaOH 0.1 mol L $^{-1}$ are shown.

Table 1

Percentages in mass (% m/m) of the elements found in BPC before and after adsorption process (obtained by XRF)

Element	BPC	BPC-adsorption
K	35.42	1.63
Ca	27.19	0.83
S	11.32	0.93
Fe	6.96	0.26
Si	5.07	0.52
Al	4.82	–
P	4.50	0.40
Zn	1.84	10.69
Cu	1.78	29.21
Cl	1.11	0.10
Pb	–	37.40
Cd	–	7.55
Ni	–	10.51

CPB before and after chemical treatment were obtained with a magnification of 500 \times and a particle size within the range of a 20–59 mesh (see Fig. 2). Both samples demonstrated a heterogeneous surface with variable pore sizes, and the particles in the raw sample were more highly aggregated than in the treated fibre. Fig. 3 shows two cashew samples following the partial removal of the lignin with an alkaline solution. This treatment increased the surface area and improved the ion retention by the cashew matrix.

3.2. Column adsorption

3.2.1. Adsorbent characterisation and flow rate and bed height effects

The physical properties of the column containing the adsorbent are shown in Table 2. The data indicate

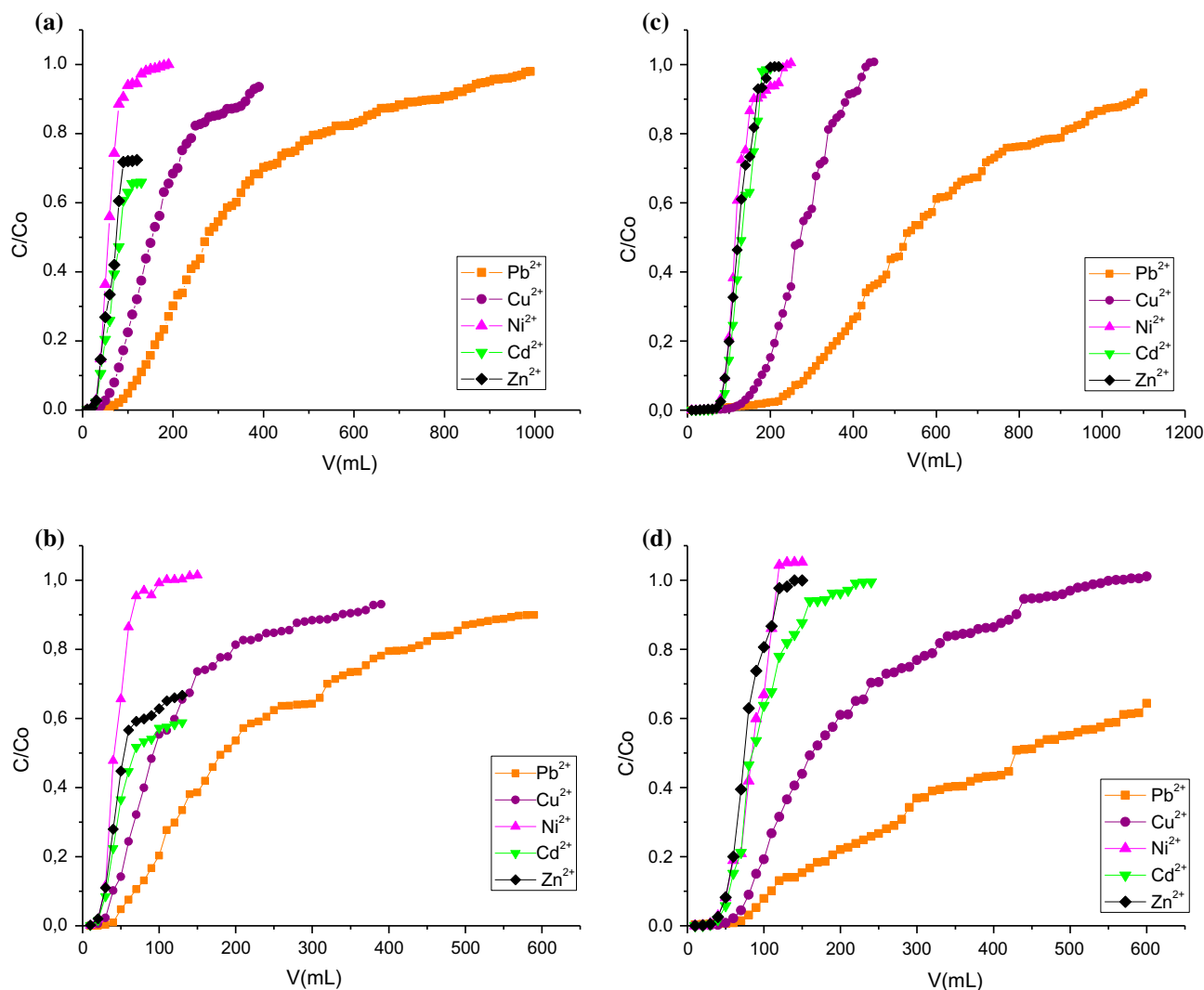


Fig. 3. Breakthrough curves for metal ions on cashew peduncle bagasse with a fixed bed height and flow rate for the adsorption of Pb^{2+} , Cu^{2+} , Ni^{2+} , Cd^{2+} and Zn^{2+} . (a) Flow rate of 3.0 mL min^{-1} and a bed height of 8.0 cm ; (b) flow rate of 6.0 mL min^{-1} and a bed height of 8.0 cm ; (c) Flow rate of 3.0 mL min^{-1} and a bed height of 12.0 cm ; (d) flow rate of 6.0 mL min^{-1} and a bed height of 12.0 cm . A multi-element model solution with a concentration of 100.0 mg L^{-1} and a pH of 5.0 was evaluated at room temperature ($28 \pm 2^\circ\text{C}$).

that the packing density was less than 8.8% and that the porosity was greater than 85% . Normally, a lower packing density leads to a greater porosity of the bed.

The effect of bed height (mass of adsorbent) on the adsorption of metal ions was investigated at an approximate ion concentration of 100.0 mg L^{-1} . Bed heights of 8.0 and 12.0 cm , representing a mass of 1.50 and 2.50 g of the treated CPB, respectively, were tested. The breakthrough curves plotted for each bed height are shown in Fig. 3(a)–(d).

An increased bed height corresponds to a greater column adsorption capacity. According to the

literature, a greater bed height correlates with a longer service time in the column due to the increased superficial area and the amount of active sites available for binding in the adsorbent [33]. Accordingly, as the bed height increased, the maximum adsorption capacity of the column increased. Thus, a bed height of 12.0 cm was selected for further analysis of the breakthrough curves.

Tests were performed to determine the optimal flow rate for the removal of metal ions using flow rates of 3.0 and 6.0 mL min^{-1} at a constant bed height of 12.0 cm (equivalent mass of 2.50 g CPB treated). The breakthrough curves obtained from a

Table 2

Physical parameters of the column bed containing the adsorbent. Hydraulic detention time (HDT), observed in the system of the column, in different flows (Initial concentration: 100.0 mg L⁻¹ of multi-component model solution; pH 5.0; bed height 12.0 cm)

Properties	Cashew peduncle bagasse
Column diameter (d _L) (cm)	1.10
Bed height (cm)	8.0;12.0
Total area of the column (cm ²)	105.5
Volume of the empty column (V _L) (cm ³)	28.50
Mass of adsorbent in the column (g)	2.50
Bulk density (g cm ³)	0.596
Packing density (g cm ³)	0.087
Particle volume (V _{ap}) (cm ³)	4.19
Porosity of the bed (%)	0.853
Flow (mL min ⁻¹)	3.0; 6.0
Hydraulic load (mL min ⁻¹ cm ⁻²)	3.16; 6.31
HDT (min)	366.6; 83.33

multi-element solution are shown in Fig. 3. It should be noted that both the volume and the volume of rupture saturation decreased significantly when the flow rate was increased from 3.0 to 6.0 mL min⁻¹. This behaviour is because the increased flow rate caused a decrease in the residence time of the metal ions in the adsorbent bed, which consequently decreased the removal efficiency of metal ions present in the solution. Thus, decreasing the flow volume effectively increased the time of column breakthrough and the treatment time of the bed, as anticipated [34]. This was especially the case for the removal of Pb²⁺, indicating that a larger solution volume could be treated. This observation was also noted for Cu²⁺, as shown in Fig. 3. The results presented in Table 2 revealed that the hydraulic detention time (HDT) increased from 83.3 to 366.6 min, thereby decreasing the time required to achieve column breakthrough. It is important to note that a greater hydraulic loading is associated with decreased adsorption due to the reduced contact time between the adsorbent and the adsorbate [29].

3.2.2. Breakthrough curves for single- and multi-element solutions

With the operating conditions optimised for the column (bed height of 12.0 cm and a flow rate of 3.0 mL min⁻¹), experiments were conducted to determine the column adsorption performance with a solution having an initial concentration of 100.0 mg L⁻¹.

The breakthrough curves for single solutions of the each metallic ion, treated with CPB, are shown in Fig. 4. The values of C_b, C_x, V_b and V_x for single- and

multi-metal systems are given in Table 3. These values were then used to calculate t_x, t_δ, t_f, f and per cent saturation at the breakpoint (Table 3).

In a single-element system, the time to move the PAZ (t_x) was the longest for Pb²⁺ (500 min) and the shortest for Ni²⁺ (170 min); Cu²⁺, Cd²⁺ and Zn²⁺ demonstrated intermediate t_x values. The time required to move the adsorption zone down in the column (t_δ) ranged from 95 to 195 min. The time required for the initial formation of the PAZ (t_f) ranged from 51 to 98 min. The fractional capacities of the

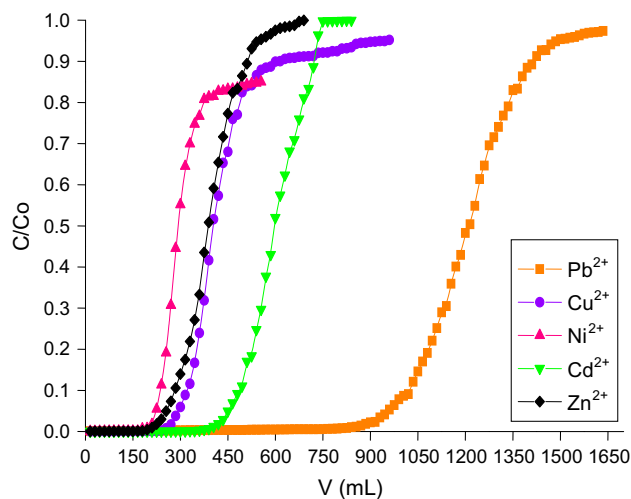


Fig. 4. Breakthrough curves for Pb²⁺, Cu²⁺, Ni²⁺, Cd²⁺ and Zn²⁺ using cashew peduncle bagasse on the column (single-element system). The initial solution concentration was 100 mg L⁻¹ at a pH of 5.0. The experiment was conducted with a flow rate of 3.0 mL min⁻¹ and a bed height of 12.0 cm at room temperature (28 ± 2°C).

Table 3

Parameters obtained from breakthrough curves. Condition: 3 mL min⁻¹ flow rate, bed height 12.0 cm, pH 5.0 at ambient temperature (28 ± 2°C)

Metal ion	C _b (mg L ⁻¹)	C _x (mg L ⁻¹)	V _b (mL)	V _x (mL)	F _m (mL min ⁻¹)	t _x (min)	t _δ (min)	t _f (min)	f	δ (cm)	Saturation (%)
<i>Single-element (synthetic effluent)</i>											
Pb ²⁺	4.47	79.65	915	1,500	3.0	500	195	98	0.496	5.8	75.52
Cu ²⁺	4.67	73.54	300	855	3.0	285	185	96	0.484	11.7	49.64
Ni ²⁺	5.01	77.72	225	510	3.0	170	95	52	0.448	9.7	55.46
Cd ²⁺	4.89	98.95	450	750	3.0	250	100	52	0.480	6.1	73.76
Zn ²⁺	4.40	84.90	255	555	3.0	185	100	51	0.491	9.0	62.07
<i>Multi-element (synthetic effluent)</i>											
Pb ²⁺	3.22	62.21	240	1,060	3.0	353	273	74	0.728	11.8	73.41
Cu ²⁺	2.74	58.97	150	400	3.0	133	83	40	0.517	10.7	56.75
Ni ²⁺	2.55	70.59	80	160	3.0	53	27	13	0.500	8.0	66.75
Cd ²⁺	3.16	51.33	90	140	3.0	47	17	8	0.507	5.2	78.71
Zn ²⁺	2.20	74.07	80	150	3.0	50	23	13	0.452	7.5	65.66
<i>Multi-element (real effluent)</i>											
Cu ²⁺	18.03	53.10	10	30	3.0	10	7	2	0.695	10.13	50.1
Ni ²⁺	1.500	3.500	10	30	3.0	10	7	3	0.500	12	50.1
Zn ²⁺	2.200	49.30	170	650	3.0	217	160	57	0.647	12	64.7

column (*f*) in the adsorption zone at the breakpoint were 0.496, 0.484, 0.448, 0.480 and 0.491 for Pb²⁺, Cu²⁺, Ni²⁺, Cd²⁺ and Zn²⁺, respectively. The per cent saturation observed from highest to lowest was: Pb²⁺ > Cd²⁺ > Zn²⁺ > Ni²⁺ > Cu²⁺.

In a multi-metal system, Fig. 3(c), the saturation volumes were lower than those for single ions. The time to establish the PAZ (*t_x*) was the longest for Pb²⁺ (353 min) and the shortest for Cd²⁺ (47 min); Cu²⁺, Ni²⁺ and Zn²⁺ demonstrated intermediate *t_x* values. The time required to shift the adsorption zone down the column (*t_δ*) ranged from 17 to 273 min. The time required for the initial formation of the PAZ (*t_f*) ranged from 8 to 74 min. The

fractional capacities of the column (*f*) in the adsorption zone at the breakpoint were 0.728, 0.517, 0.500, 0.507 and 0.452 for Pb²⁺, Cu²⁺, Ni²⁺, Cd²⁺ and Zn²⁺, respectively (Table 3).

The per cent saturations for the metal ions on the column were observed in the following order: Cd²⁺ > Pb²⁺ > Ni²⁺ > Zn²⁺ > Cu²⁺. The results demonstrated that the greatest percentage of saturation was obtained for Cd²⁺ using a short adsorption zone length, whereas for the other ions, the presence of a longer adsorption zone increased the per cent saturation. The literature has reported that a smaller adsorption zone (*δ*) and high fractional rate (*f*) corresponded to the most efficient removal.

Table 4

Comparison of adsorption capacity of Pb²⁺, Cu²⁺, Ni²⁺, Cd²⁺ and Zn²⁺ with several biosorbents to system of fixed bed

Adsorbent	Q (mg g ⁻¹)					pH	Flow (mL min ⁻¹)	Bed height (cm)	References
	Pb ²⁺	Cu ²⁺	Ni ²⁺	Cd ²⁺	Zn ²⁺				
Cashew peduncle (metal single)	49.71	25.83	16.86	28.58	19.43	5	3	12	This work
Cashew peduncle (metal multi)	29.83	10.63	4.74	3.59	4.10	5	3	12	This work
Green coconut shell (metal single)	54.62	41.36	16.34	37.78	17.08	5	2	10	[35]
Green coconut shell (metal multi)	17.90	20.26	3.12	11.96	7.32	5	2	10	[35]
<i>Sphagnum</i> peat moss	–	–	5.41	8.15	–	3.9	1.5	15	[36]
Tea waste	65.00	48.00	–	–	–	5–6	20	10	[37]
<i>Paenibacillus polymyxa</i>	–	69.02	62.80	–	–	5	1.5	6	[38]
SWC Calcium–alginate beads	–	–	–	23.6	–	6	1	30	[39]
<i>Tamarindus</i>	–	110.472	–	–	–	6	10	12	[40]
Expanding rice husk	–	5.838	–	–	–	5.45	10	9	[41]
Tururi Fibers	6.30	16.30	6.40	18.20	–	5.5	1	9.5	[42]

The adsorption capacity results obtained for the adsorption of toxic metal ions from single- and multi-metal ion solutions on CPB for fixed-bed column systems are compared with other types of waste biomass used for the adsorption treatment of aqueous solutions containing toxic metals in Table 4 [35–42]. As illustrated in Table 4, the CPB demonstrated good adsorption capacity when compared to other adsorbents. This result may be related to the experimental conditions employed as well as to the affinity of the metal ions for the functional groups present on the adsorbent surface.

In this study, we verified the feasibility and potential use of treated cashew bagasse as an inexpensive, effective and readily available material that can be

used in place of commercially available conventional adsorbents for the treatment of industrial effluents. However, a direct comparison between the adsorbents is difficult due to the use of different experimental conditions across studies.

3.2.3. Thomas model

A successful design of a column ion-exchange process requires prediction of the concentration–time profile for the effluent. The maximum adsorption capacity of an adsorbent is also required for design of this process. The Thomas model was applied to the experimental data obtained for synthetic multi-metal

Table 5
Predicted parameters from Thomas model for multi-metal ions adsorption on cashew peduncle bagasse

	Flow rate (mL min ⁻¹)		Bed height (8.0 cm)		Bed height (12.0 cm)	
			Non linear	Linear	Non linear	Linear
Pb ²⁺	3.0	K _t	1.79 × 10 ⁻⁴	1.85 × 10 ⁻⁴	3.17 × 10 ⁻⁴	3.19 × 10 ⁻⁴
		q ₀	1.77	1.61	1.69	1.84
		SSE	8.46 × 10 ⁻¹⁴	6.15	0.00	26.88
	6.0	K _t	3.32 × 10 ⁻⁴	3.67 × 10 ⁻⁴	2.29 × 10 ⁻⁴	2.28 × 10 ⁻⁴
		q ₀	1.31	1.07	2.55	2.82
		SSE	3.75 × 10 ⁻¹⁷	10.02	0.00	29.79
Cu ²⁺	3.0	K _t	4.68 × 10 ⁻⁴	4.77 × 10 ⁻⁴	1.31 × 10 ⁻³	1.31 × 10 ⁻³
		q ₀	8.63	7.75	7.18	7.37
		SSE	1.91 × 10 ⁻¹⁴	2.14	7.70 × 10 ⁻³⁰	0.518
	6.0	K _t	5.24 × 10 ⁻⁴	5.06 × 10 ⁻⁴	9.08 × 10 ⁻⁴	9.07 × 10 ⁻⁴
		q ₀	5.91	5.63	9.03	9.09
		SSE	6.94 × 10 ⁻²	0.0767	1.28 × 10 ⁻¹³	17.59
Ni ²⁺	3.0	K _t	1.77 × 10 ⁻³	1.79 × 10 ⁻⁴	3.10 × 10 ⁻³	3.10 × 10 ⁻³
		q ₀	3.09	2.90	3.49	3.85
		SSE	8.51 × 10 ⁻¹⁴	0.108	1.97 × 10 ⁻³¹	1.41
	6.0	K _t	5.24 × 10 ⁻³	5.06 × 10 ⁻⁴	5.19 × 10 ⁻³	5.32 × 10 ⁻³
		q ₀	5.91	5.63	3.44	1.86
		SSE	2.03	1.08	7.40 × 10 ⁻³¹	15.42
Cd ²⁺	3.0	K _t	1.50 × 10 ⁻⁴	1.50 × 10 ⁻⁴	3.67 × 10 ⁻³	3.67 × 10 ⁻³
		q ₀	4.62	4.74	3.13	3.23
		SSE	3.32 × 10 ⁻¹⁵	0.040	1.97 × 10 ⁻³¹	1.41
	6.0	K _t	5.24 × 10 ⁻³	5.06 × 10 ⁻⁴	4.13 × 10 ⁻³	4.19 × 10 ⁻³
		q ₀	5.91	5.63	4.36	2.36
		SSE	4.02 × 10 ⁻¹	13.03	3.70 × 10 ⁻¹³	17.39
Zn ²⁺	3.0	K _t	1.89 × 10 ⁻³	1.89 × 10 ⁻³	3.37 × 10 ⁻³	3.37 × 10 ⁻³
		q ₀	4.09	4.18	3.13	3.48
		SSE	1.82 × 10 ⁻¹⁶	0.03	1.2310 ⁻³²	0.01
	6.0	K _t	1.81 × 10 ⁻³	1.81 × 10 ⁻³	5.48 × 10 ⁻³	5.48 × 10 ⁻³
		q ₀	6.73	7.25	3.45	3.59
		SSE	1.48 × 10 ⁻¹⁶	0.54	8.39 × 10 ⁻³¹	0.10

ion solutions percolated through the column at a flow rate of 3 to 6 mL min⁻¹ and a bed height of 8 to 12 cm.

Nonlinear regression analysis was performed using the sum of squared errors (SSE) for every experimental data-set. The values of K_t and q_0 were determined using the lowest error values in each case, by adjusting and optimising the functions themselves using the *solver* add-in for Microsoft Excel[®]. The values of K_t and q_0 obtained using the lowest error values are shown in Table 5. The SSE is given by Eq. 10 [43]:

$$\text{SSE} = \sum_{i=1}^p (q_e - q_{\text{cal}})^2 \quad (10)$$

where q_e is the adsorption capacity determined from the column data, q_{cal} is the estimated adsorption capacity and p is the number of parameters in the

regression model. A smaller function value indicates the best curve-fitting.

Application of the Thomas model revealed that it did not fit the experimental data well, except for experiments with a bed height of 12.0 cm and a flow rate of 3.0 mL min⁻¹, as observed for Cu²⁺ (Fig. 5). For these optimal conditions, the experimental data were well-described by the Thomas model for all of the metal ions studied.

The nonlinear regression (NL) analysis represents the theoretical data more accurately than the linear regression analysis (L). As reported in Table 5, the model errors for NL were lower than for L, demonstrating a better model fit.

According to the data presented in Table 5, increasing the flow rate from 3 to 6 mL min⁻¹ increased the Thomas rate constant (K_t) by 1.1, 1.9, 2.9 and 3.5-fold-control for Cu²⁺, Pb²⁺, Ni²⁺ and Cd²⁺, respectively, likely because the adsorption rate of

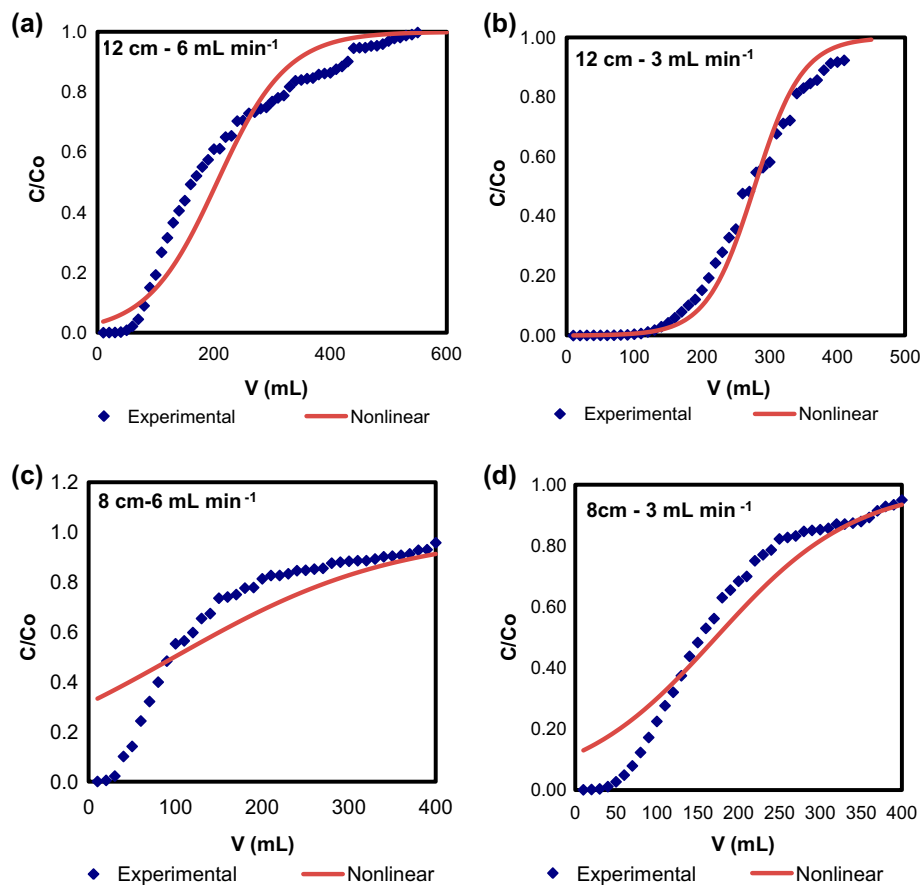


Fig. 5. Experimental and predicted data from Thomas model (nonlinear) for Cu²⁺ adsorption in a fixed bed and flow rate on cashew peduncle bagasse: (a) 6 mL min⁻¹ flow rate, bed height 12.0 cm, (b) 3 mL min⁻¹ flow rate, bed height 12.0 cm, (c) 6 mL min⁻¹ flow rate, bed height 8.0 cm, and (d) 3 mL min⁻¹ flow rate, bed height 8.0 cm.

metal ion transfer from the solution to the fixed-bed column was primarily driven by flow rate [44].

It should also be noted that adsorption capacity for some metal ions decreased with increased bed height (Table 5). Copper and lead ion adsorption increased with increased flow, whereas for nickel, cadmium and zinc ions the adsorption capacity decreased. K_t represents the rate mass transfer of metal ions from the solution to the CPB and was observed for the ions in the following order: $Cd > Zn > Ni > Cu > Pb$. In contrast, the rate of mass transfer for multi-metal solutions followed the order of adsorption capacity: $Pb > Cu > Ni > Zn > Cd$, highlighting both the effects of metal ion competition and the affinities of Pb and Cu for adsorbent sites.

3.2.4. Breakthrough curves for an electroplating industry effluent

The same tests performed to characterise the breakthrough curves of multi-metal systems were also performed using an effluent sample from the electroplating industry that contained Cu^{2+} (61.16 mg L^{-1}), Ni^{2+} (3.97 mg L^{-1}) and Zn^{2+} (47.70 mg L^{-1}). The experimental conditions were optimised for fixed-bed biosorption, and the results are reported in Table 3. When the pH was changed to 5.0, saturation occurred at volumes of 30 mL for Cu^{2+} and 650 mL for Zn^{2+} . The behaviour of the breakthrough event was different when compared to the synthetic effluent samples, and this may have resulted from competition with others

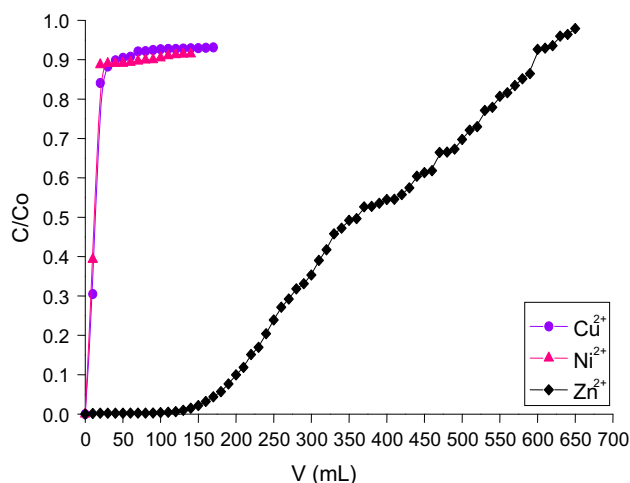


Fig. 6. Breakthrough curves of a real effluent sample using cashew peduncle bagasse at a pH of 5. Experiments were conducted with a flow rate of 3.0 mL min^{-1} , bed height of 12.0 cm and at room temperature ($28 \pm 2^\circ\text{C}$).

metal ions, e.g. Pb^{2+} . The saturation volume of Ni^{2+} was not changed. The values of C_b , C_x , V_b and V_x as interpolated from the data presented in Fig. 6, were used to calculate t_x , t_δ , t_f , f and the per cent saturation at the breakthrough event.

The total time to establish the PAZ (t_x) ranged from 10 to 217 min. The time required to move the adsorption zone down the column (t_δ) and the time required for the initial formation of the PAZ (t_f) ranged from 7 to 160 and 2 to 57 min, respectively. The adsorption capacities increased to 0.132, 5.96 and 42.50 mg g^{-1} for Ni^{2+} , Zn^{2+} and Cu^{2+} , respectively.

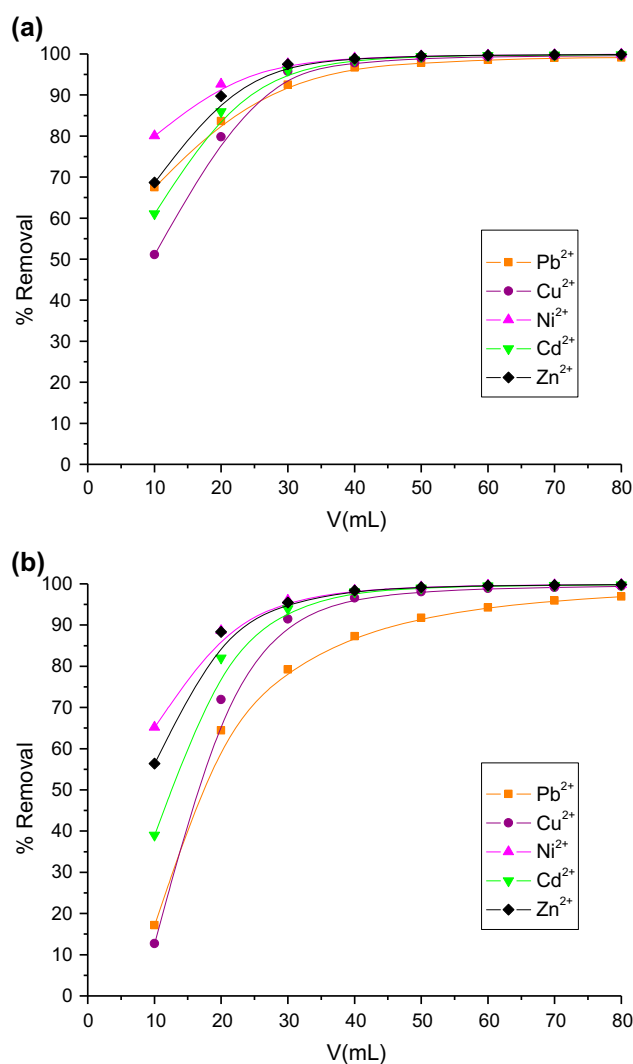


Fig. 7. Percent desorption of metal ions from the column using acid eluents HCl (mol L^{-1}) (a) and HNO_3 (mol L^{-1}) (b). A model multi-element solution with an initial concentration of 100 mg L^{-1} at a pH of 5.0 was used with a flow rate of 3.0 mL min^{-1} and a bed height of 12.0 cm at room temperature ($28 \pm 2^\circ\text{C}$).

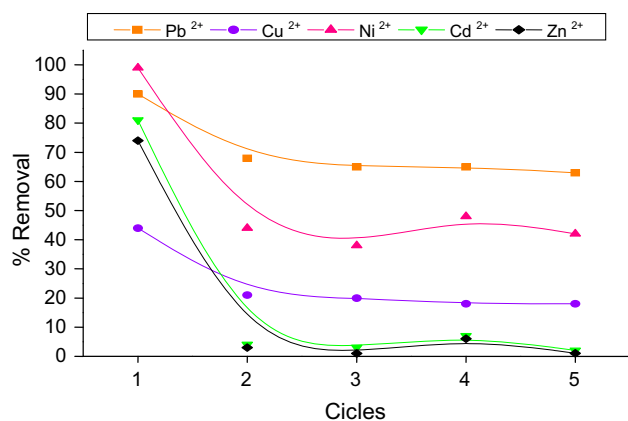


Fig. 8. Efficiency of removal of metals as a function of the number of cycles of column reuse with cashew peduncle bagasse as the adsorbent. A model multi-element solution with an initial concentration of 100 mg L^{-1} at a pH of 5.0 was used with a flow rate of 3.0 mL min^{-1} and a bed height of 12.0 cm at room temperature ($28 \pm 2^\circ\text{C}$).

The percentage of saturation at pH of 1.14 was approximately 50% for all metal ions, whereas at pH of 5, 83.42% saturation was observed for Ni^{2+} , 71.45% for Zn^{2+} and 56.40% for Cu^{2+} . It may be concluded that at a pH of 5 the competitive effects of protons for active sites on the adsorbent were diminished.

3.2.5. Column regeneration and recycling of the column

A column bed depth of 12.0 cm and a flow rate of 3.0 mL min^{-1} were selected for this study. Desorption flow experiments were conducted after column saturation with a multi-metal ion solution, and the results are shown in Fig. 7.

Metal ion desorption was carried out by an acid elution method using HCl (1.0 mol L^{-1}) and HNO_3 (1.0 mol L^{-1}) as shown in Fig. 7. An optimal eluent would elute all of the ions using a low volume [35]. Our results demonstrated that both acids removed all metal ions using 50 mL of acid solution. However, due to the low cost of HCl , it was chosen for studies of column regeneration.

After the adsorption and desorption experiments, tests were conducted to evaluate whether the column could be recycled. The results following five regeneration cycles are shown in Fig. 8. It was observed that reuse of the adsorbent decreased the removal efficiency for all metal ions when compared to the first cycle. The removal capacities were reduced more than 90% for Pb^{2+} , 44% for Cu^{2+} , 99% for Ni^{2+} , 81% for Cd^{2+} and 74% for Zn^{2+} .

4. Conclusions

Single- and multi-metal ion removal was improved by batch processing of column adsorption. The breakthrough capacities using cashew peduncle bagasse for the adsorption of single- and multi-metal ion solutions containing Pb^{2+} , Cu^{2+} , Ni^{2+} , Cd^{2+} and Zn^{2+} were 49.71, 35.83, 16.86, 39.58 and 29.43 mg g^{-1} , and 29.83, 14.63, 6.740, 4.590 and 5.100 mg g^{-1} , respectively.

The maximal adsorption efficiency of cashew peduncle bagasse was demonstrated by eluting Pb^{2+} , Cu^{2+} , Ni^{2+} , Cd^{2+} and Zn^{2+} from exhausted columns. We observed that 100% of the metal ions, except for Pb^{2+} , could be recovered when 40 mL of 0.1 mol L^{-1} HCl or HNO_3 were used as the eluent.

Adsorbent regeneration decreased the removal efficiency for all of the metal ions in the first cycle; however, the recovery of metal ions from small effluent volumes suggests that CPB is an economical adsorbent for a simple disposal method of preconcentrated metal ions.

Acknowledgements

The authors would like to thank FUNCAP (Fundação Cearense de Pesquisa,) and CNPq (Conselho Nacional de Desenvolvimento Científico e Tecnológico. We also thank the Laboratory of Trace Analysis and Laboratory of Water Analysis of the Federal University of Ceará, as well as EMBRAPA-Tropical Agro-industry, CE, Brazil (EMBRAPA/CE) for samples of cashew peduncle bagasse.

References

- [1] G. McKay, Use of Adsorbents for the Removal of Pollutants from Wastewaters, CRC Press, Boca Raton, FL, 1996.
- [2] D.O. Cooney, Adsorption Design for Wastewater Treatment, CRC Press, Boca Raton, FL, 1999.
- [3] D.M. Ruthven, Principles of Adsorption and Adsorption Process, Wiley, New York, NY, 1984.
- [4] H. Muhamad, H. Doan, A. Lohi, Batch and continuous fixed-bed column biosorption of Cd^{2+} and Cu^{2+} , Chem. Eng. J. 158 (2010) 369–377.
- [5] V.K. Thakur, M.K. Thakur, P. Raghavan, M.R. Kessler, Progress in green polymer composites from lignin for multifunctional applications: A review, Acs Sustain. Chem. Eng. 2(5) (2014) 1072–1092.
- [6] V.K. Thakur, M.K. Thakur, Processing and characterization of natural cellulose fibers/thermoset polymer composites, Carbohydr. Polym. 109 (2014) 102–117.
- [7] V.K. Thakur, M.K. Thakur, R.K. Gupta, Review: Raw natural fiber-based polymer composites, Int. J. Polym. Anal. Charact. 19 (2014) 256–271.

- [8] G. Annadurai, R.S. Juang, D.J. Lee, Adsorption of heavy metals from water using banana and orange peels, *Water Sci. Technol.* 47 (2003) 185–190.
- [9] A.C.H. Barreto, M.M. Costa, A.S.B. Sombra, D.S. Rosa, R.F. Nascimento, S.E. Mazzetto, P.B.A. Fechine, Chemically modified banana fiber: Structure, dielectrical properties and biodegradability, *J. Polym. Environ.* 18 (2010) 523–531.
- [10] V.S.O. Neto, T.V. Carvalho, S.B. Honorato, C.L. Gomes, F.C. Freitas, A.A.M. Silva, P.T.C. Freire, R.F. Nascimento, Coconut bagasse treated by thiourea/ammonia solution for cadmium removal: kinetics and adsorption equilibrium, *Bioresources* 7 (2012) 1504–1524.
- [11] P.C. Okafor, P.U. Okon, E.F. Daniel, E.E. Ebenso, Adsorption capacity of coconut (*Cocos nucifera* L.) shell for lead, copper, cadmium and arsenic from aqueous solutions, *Int. J. Electrochem. Sci.* 7 (2012) 12354–12369.
- [12] G.H. Pino, L. Souza de Mesquita, M.L. Torem, G.A. Saavedra Pinto, Biosorption of cadmium by green coconut shell powder, *Miner. Eng.* 19 (2006) 380–387.
- [13] V.O.S. Neto, D.Q. Melo, T.C. Oliveira, R.N.P. Teixeira, M.A.A. Silva, R.F. Nascimento, Evaluation of new chemically modified coconut shell adsorbents with tannic acid for Cu (II) removal from wastewater, *J. Appl. Polym. Sci.* 131 (2014) 40744-1–40744-12, doi: [10.1002/app.40744](https://doi.org/10.1002/app.40744).
- [14] V.C.G. Dos Santos, J.V.T.M. De Souza, C.R.T. Tarley, J. Caetano, D.C. Dragunski, Copper ions adsorption from aqueous medium using the biosorbent sugarcane bagasse in nature and chemically modified, *Water Air Soil Pollut.* 216 (2011) 351–359.
- [15] F.W. Sousa, M.J. Sousa, I.R.N. Oliveira, A.G. Oliveira, R.M. Cavalcante, P.B.A. Fechine, Evaluation of a low cost adsorbent for removal of toxic metal ions from wastewater of an electroplating factory, *J. Environ. Manage.* 90 (2009) 3340–3344.
- [16] O.K. Junior, A.L.V. Gurgel, J.C.P. Melo, V.R. Botaro, T.M.M. Sacramento, R.P.F. Gil, L. Frederic Gil, Adsorption of heavy metal ion from aqueous single metal solution by chemically modified sugarcane bagasse, *Bioresour. Technol.* 98 (2007) 1291–1297.
- [17] S.A. Moreira, F.W. Sousa, A.G. Oliveira, R.F. Nascimento, E.S. Brito, Estudo da remoção de metais pesados por bagaço de caju (Metal removal from aqueous solution using cashew bagasse), *Quim. Nova* 32 (2009) 1717–1722.
- [18] R.F. Nascimento, F.W. Sousa, V.O.S. Neto, P.B.A. Fechine, R.N.P. Teixeira, P.T.C. Freire, M.A. Araujo-Silva, Biomass adsorbent for removal of toxic metal ions from electroplating industry wastewater, in: Darwin Sebayang (Ed.), *Electroplating*, InTech, Rijeka, 2012, pp. 101–136.
- [19] R.P. Santos, A. Santiago, C. Gadelha, J.B. Cajazeiras, B.S. Cavada, J.L. Martins, T. Oliveira, G. Bezerra, R.P. Santos, V.N. Freire, Production and characterization of the cashew (*Anacardium occidentale* L.) peduncle bagasse ashes, *J. Food Eng.* 79 (2007) 1432–1437.
- [20] Ö. Can, D. Balköse, S. Ülkü, Batch and column studies on heavy metal removal using a local zeolitic tuff, *Desalination* 259 (2010) 17–21.
- [21] C. Li, P. Champagne, Fixed-bed column study for the removal of cadmium (II) and nickel (II) ions from aqueous solutions using peat and mollusk shells, *J. Hazard. Mater.* 171 (2009) 872–878.
- [22] I.A. Aguayo-Villarreal, A. Bonilla-Petriciolet, V. Hernández-Montoya, M.A. Montes-Morán, H.E. Reynel-Avila, Batch and column studies of Zn²⁺ removal from aqueous solution using chicken feathers as sorbents, *Chem. Eng. J.* 167 (2011) 67–76.
- [23] M. Sobhy, E. Yakout, H. Borai, Adsorption behavior of cadmium onto natural chabazite: batch and column investigations, *Desalin. Water Treat.* 52 (2014) 4212–4222.
- [24] A. Bhatnagar, V.J.P. Vilar, C.M.S. Botelho, R.A.R. Boaventura, Coconut—based biosorbents for water treatment. A review of the recent literature, *Adv. Colloid Interface Sci.* 160 (2010) 1–15.
- [25] J. Febrianto, A.N. Kosasih, J. Sunarso, Y.-H. Ju, N. Indraswati, S. Ismadi, Equilibrium and kinetic studies in adsorption of heavy metals using biosorbent: A summary of recent studies, *J. Hazard. Mater.* 162 (2009) 616–645.
- [26] T.A.H. Nguyen, H.H. Ngo, W.S. Guo, J. Zhang, S. Liang, Q.Y. Yue, Q. Li, T.V. Nguyen, Applicability of agricultural waste and by-products for adsorptive removal of heavy metals from wastewater, *Bioresour. Technol.* 148 (2013) 574–585.
- [27] V.K. Thakur, A.S. Singha, Physico – chemical and mechanical characterization of natural fiber reinforced polymer composites, *Iran. Polym. J.* 19(1) (2010) 3–16.
- [28] V.K. Thakur, A.S. Singha, B.N. Misra, Graft copolymerization of methyl methacrylate onto cellulosic biofibers, *J. Appl. Polym. Sci.* 122 (2011) 532–544.
- [29] A.G. Oliveira, J.P. Ribeiro, D.Q. Melo, F.W. Sousa, V.O. Sousa Neto, G.S.C. Raulino, R.M. Cavalcante, R.F. Nascimento, Evaluation of two biosorbents in the removal of metal ions in aqueous using a pilot scale fixed-bed system, *Orbital: Electron. J. Chem.* 6 (2014) 47–55.
- [30] G.S.C. Raulino, C.B. Vidal, A.C.A. Lima, D.Q. Melo, J.T. Oliveira, R.F. Nascimento, Treatment influence on green coconut shells for removal of metal ions: Pilot-scale fixed-bed column, *Environ. Technol.* 35 (2014) 1711–1720.
- [31] H.C. Thomas, Heterogeneous ion exchange in a flowing system, *J. Am. Chem. Soc.* 66 (1944) 1664–1666.
- [32] Á.G. Paulino, A.J. da Cunha, R.V.S. da Silva Alfaya, A.A.S. da Silva Alfaya, Chemically modified natural cotton fiber: A low-cost biosorbent for the removal of the Cu(II), Zn(II), Cd(II), and Pb(II) from natural water, *Desalin. Water Treat.* 52 (2014) 4223–4233.
- [33] R. Han, W. Zou, H. Li, Y. Li, J. Shi, Copper(II) and lead(II) removal from aqueous solution in fixed-bed columns by manganese oxide coated zeolite, *J. Hazard. Mater.* 137 (2006) 934–942.
- [34] G. Xiao, X. Zhang, H. Su, T. Tan, Plate column biosorption of Cu(II) on membrane-type biosorbent (MBS) of *Penicillium biomass*: Optimization using statistical design methods, *Bioresour. Technol.* 143 (2013) 490–498.
- [35] F.W. Sousa, M.J.B. Silva, I.R.N. Oliveira, A.G. Oliveira, R.M. Cavalcante, P.B.A. Fechine, V.O. Sousa Neto, D. Keukeleire, R. F. Nascimento, Evaluation of a low cost adsorbent for removal of toxic metal ions from wastewater of an electroplating factory, *J. Environ. Manage.* 1 (2009) 1–5.

- [36] P. Champagne, C. Li, Use of Sphagnum peat moss and crushed mollusk shells in fixed-bed columns for the treatment of synthetic landfill leachate, *J. Mater. Cycles Waste Manage.* 11 (2009) 339–347.
- [37] B.M.W.P.K. Amarasinghe, R.A. Williams, Tea waste as a low cost adsorbent for the removal of Cu and Pb from wastewater, *Chem. Eng. J.* 132 (2007) 299–309.
- [38] F. Çolak, A. Olgun, N. Atar, D. Yazıcıoğlu, Heavy metal resistances and biosorptive behaviors of *Paenibacillus polymyxa*: Batch and column studies, *J. Ind. Eng. Chem.* 19 (2013) 863–869.
- [39] M. Jain, V.K. Garg, K. Kadirvelu, Cadmium(II) sorption and desorption in a fixed bed column using sunflower waste carbon calcium–alginate beads, *Bioresour. Technol.* 129 (2013) 242–248.
- [40] S. Chowdhury, P. Saha, Batch and continuous (fixed-bed column) biosorption of Cu(II) by *Tamarindus indica* fruit shell, *Korean J. Chem. Eng.* 30 (2013) 369–378.
- [41] X. Luo, Z. Deng, X. Lin, C. Zhang, Fixed-bed column study for Cu²⁺ removal from solution using expanding rice husk, *J. Hazard. Mater.* 187 (2011) 182–189.
- [42] D.Q. Melo, C.B. Vidal, A.L. Silva, R.N.P. Teixeira, G.S.C. Raulino, T.C. Medeiros, P.B.A. Fechine, S.E. Mazzeto, D. Keukeleire, R.F. Nascimento, Removal of Cd²⁺, Cu²⁺, Ni²⁺, and Pb²⁺ ions from aqueous solutions using tururi fibers as an adsorbent, *J. Appl. Polym. Sci.* 131 (2014) 40883-1–40883-12. doi: [10.1002/app.40883](https://doi.org/10.1002/app.40883).
- [43] D.Q. Melo, V.O.S. Neto, J.T. Oliveira, A.L. Barros, E.C.C. Gomes, G.S.C. Raulino, E. Longuinotti, R.F. Nascimento, Adsorption equilibria of Cu²⁺, Zn²⁺, and Cd²⁺ on EDTA-functionalized silica spheres, *J. Chem. Eng. Data* 58 (2013) 798–806.
- [44] M. Revathi, M. Saravanan, A.B. Chiya, M. Velan, Removal of copper, nickel, and zinc ions from electroplating rinse water, *CLEAN—Soil, Air, Water* 40 (2012) 66–79.